Accurate Potential Energy Surface and Calculated Spectroscopic Properties for CdH_2 Isotopomers†

Peter Sebald,‡ Rainer Oswald, and Peter Botschwina*

Institut für Physikalische Chemie, Universität Göttingen, Tammannstrasse 6, D-37077 Göttingen, Germany

Hermann Stoll

Institut für Theoretische Chemie, Universität Stuttgart, Pfaffenwaldring 55, D-70569 Stuttgart, Germany

Detlev Figgen

Centre for Theoretical Chemistry and Physics, New Zealand Institute for Advanced Study, Massey University Albany, Auckland 0745, New Zealand

Received: March 31, 2009; Revised Manuscript Received: June 25, 2009

Ab initio calculations employing the coupled cluster method CCSD(T), in conjunction with a small-core pseudopotential for the cadmium atom, have been employed to construct a near-equilibrium potential energy function (PEF) and an electric dipole moment function (EDMF) for CdH_2. The significance of the spin−orbit interaction was checked and found to be of minor importance. Making use of two pieces of experimental information for the most abundant isotopomer $^{114}CdH_2$, we obtained a refined PEF, which, within variational calculations of rovibrational states and wave functions, reproduces all available experimental data (S. Yu, A. Shayesteh, and P. F. Bernath, *J. Chem. Phys.* **2005**, *122*, 194301) very well. In addition, numerous predictions are made. In particular, the ν_2 band origins for $^{114}CdH_2$ and $^{114}CdD_2$ are predicted at 605.9 and 436.9 cm^{-1}, respectively, and the state perturbing the e parity levels of the $(0,0^0,1)$ state of $^{114}CdH_2$ at $J = 12-17$ is identified as the $(0,3^3,0)$ state. Assignments for further perturbations found in the emission spectra are given as well.

1. Introduction

Owing to their importance in chemical synthesis as intermediates in catalytic reactions, transition metal hydrides have attracted much interest over the past few decades. The spectroscopic characterization of such species was mostly achieved by means of matrix infrared (IR) spectroscopy (see, e.g., ref 1 for a recent review). On the other hand, high-resolution spectroscopic studies involving rotational resolution, thereby enabling the acquisition of accurate structure information, are still scarce. As far as the important metal dihydrides or metal dihydrogen complexes are concerned, only FeH_2, ZnH_2, CdH_2, and HgH_2 have so far been studied by high-resolution IR spectroscopy, primarily thanks to the efforts of Bernath and co-workers.[2−7]

The topic of the present paper is a thorough theoretical investigation of the dihydride CdH_2 in its linear electronic ground state ($X^1\Sigma_g^+$). Following IR spectroscopic studies of CdH_2, CdHD, and CdD_2 in argon, neon, and hydrogen matrices,[8,9] high-resolution emission spectra of 12 symmetric isotopomers of cadmium dihydride were published by Yu et al.[6] In all cases, the ν_3 band (antisymmetric stretching mode) was observed, which corresponds to the transition between vibrational states $(v_1,v_2^l,v_3) = (0,0^0,1)$ and $(0,0^0,0)$. For the six CdH_2 isotopomers, two hot bands could be observed as well. They were assigned to the transitions $(0,0^0,2)-(0,0^0,1)$ and $(0,1^1,1)-(0,1^1,0)$. The $(0,0^0,1)$ state was found to be perturbed and some arguments were given that the $(0,3^1,0)$ state corresponds to the perturbing state. Further perturbations were noted for the $(0,1^1,1)$ and $(0,0^0,2)$ vibrational states, but no detailed analysis was possible.

The precise experimental data now available for various isotopomers of cadmium dihydride provide an excellent testing ground for the quality of current state-of-the-art ab initio calculations. To the authors' knowledge, previous quantum-chemical calculations of spectroscopic properties of CdH_2 and its isotopomers are scarce and did not go beyond the harmonic approximation. We mention the work of Green et al.[8] and Wang and Andrews,[9] which reported results of calculations carried out by second order Møller−Plesset perturbation method (MP2) and the coupled cluster method CCSD(T)[10] as well as by the hybrid density functional method B3LYP.

The present theoretical paper significantly extends and improves the previous work and attempts to make accurate predictions of spectroscopic quantities which have not yet been determined through experiment. To be more specific, we make use of a high-quality pseudopotential for the cadmium atom as developed recently[11] in conjunction with a much larger basis set than employed in previous work. In addition, rovibrational term energies and wave functions as well as transition moments among them have been calculated variationally. Particular efforts have been undertaken to elucidate the nature of the perturbations noted above.

2. Electronic Structure Calculations

2.1. Potential Energy Surfaces. CdH_2 in its electronic ground state was studied by the coupled cluster method CCSD(T) in conjunction with pseudopotentials, termed PP-

† Part of the "Walter Thiel Festschrift".

* Corresponding author. E-mail: pbotsch@gwdg.de.

‡ Permanent address: Madenburgstrasse 14, D-76865 Insheim, Germany.

10.1021/jp9029198 CCC: $40.75
Published on Web 08/05/2009

CCSD(T). A small-core energy-consistent pseudopotential (PP) was used for the central cadmium atom,[11] the core comprising the 28-electron configuration $1s^22s^22p^63s^23p^63d^{10}$. For the explicit description of the 20 valence and outer-core electrons of the Cd atom, Dunning-type correlation-consistent polarized valence *n*-tuple ζ basis sets (cc-pVnZ) were used together with functions of relevance for Cd outer-core (4sp) correlation (cc-pwCVnZ).[12] The PP-CCSD(T) calculations of the present work make use of the largest basis set available in the literature, corresponding to $n = 5$. Since the hydrogen atoms in the molecule exhibit substantial hydride character, they are described by basis sets of type aug-cc-pVnZ,[13−15] again employing $n = 5$ in the vast majority of the calculations. The complete basis set for CdH_2 at $n = 5$ comprises 366 contracted Gaussian-type orbitals (cGTOs). Throughout, all PP-CCSD(T) calculations of the present work were carried out with the MOLPRO suite of programs.[16,17] The equilibrium Cd−H distance of linear symmetric CdH_2 was obtained to be r_e(PP-CCSD(T)) = 1.666792 Å, with a corresponding total energy of −168.91953840 E_h.

In our previous work on HgH_2,[18] valence-isoelectronic to CdH_2, spin−orbit (SO) corrections were calculated explicitly by means of double-group spin−orbit configuration interaction (SO−CI) as incorporated in the program package COLUMBUS.[19,20] Although one may well expect that SO corrections are much smaller in the case of CdH_2, we have made some checks to confirm this conjecture. For this purpose, we performed double-group SO−CI calculations with and without the SO part of the Cd pseudopotential. The cc-pwCVQZ[12] and cc-pVQZ[13] basis sets were used for Cd and H, respectively; for technical reasons, we had to leave out the h functions for Cd. Like in the PP-CCSD(T) calculations described above, 22 valence and outer-core electrons were correlated in the molecule. SO−CI describes the second-order SO effects for CdH_2, together with electron correlation effects, by including all single and double excitations (CISD) from the closed-shell singlet ground state with spin symmetries up to quintet. The SO energy contribution determined this way at r_e (PP-CCSD(T)) is −0.0145325225 E_h, i.e., less than 0.01% of the scalar-relativistic CISD energy. Including the SO part of the pseudopotential changes the weight of the reference function in the CISD wave function from 0.908 to 0.907. Upon variation of a single CdH distance in the range -0.4 Å $\leq \Delta r \leq 1.0$ Å, where Δr measures the deviation from r_e(PP-CCSD(T)), the relative SO contributions change from −10.7 to +16.4 cm^{-1}. Total energy values at 15 different Δr values are available as Supporting Information. Even smaller relative contributions of less than 3 cm^{-1} are calculated when the angle to linearity is changed from 0° to 90°. From these data we may calculate a reduction of the CdH equilibrium bond length by only 0.00021 Å through the consideration of second-order SO effects. As we will see later, this difference is much smaller than the error in r_e arising from other approximations made in the PP-CCSD(T) calculations, thereby justifying the neglect of explicitly calculated SO contributions to the potential energy surface in the following.

To get some first impression of the PP-CCSD(T) potential energy surface for CdH_2 in comparison with HgH_2,[18] plots of the variation of the energy with single metal−hydrogen bond stretching (Figure 1) and with angle bending (Figure 2) were made. The underlying energy points are supplied as Supporting Information. As illustrated by the figures and strengthened by other indicators such as the T_1 diagnostics,[21] the CCSD(T) method works well up to energies of at least 15 000 cm^{-1} above equilibrium. Compared with HgH_2, the Cd−H stretching potential is significantly more shallow and its minimum is shifted to a larger r_e value by 0.0300 Å. Likewise, the H−Hg−H bending potential (see Figure 2) is much steeper than that of CdH_2, the ratio of the quadratic bending force constants $(\partial V^2/\partial\theta^2)_e$ amounting to as much as 1.602.

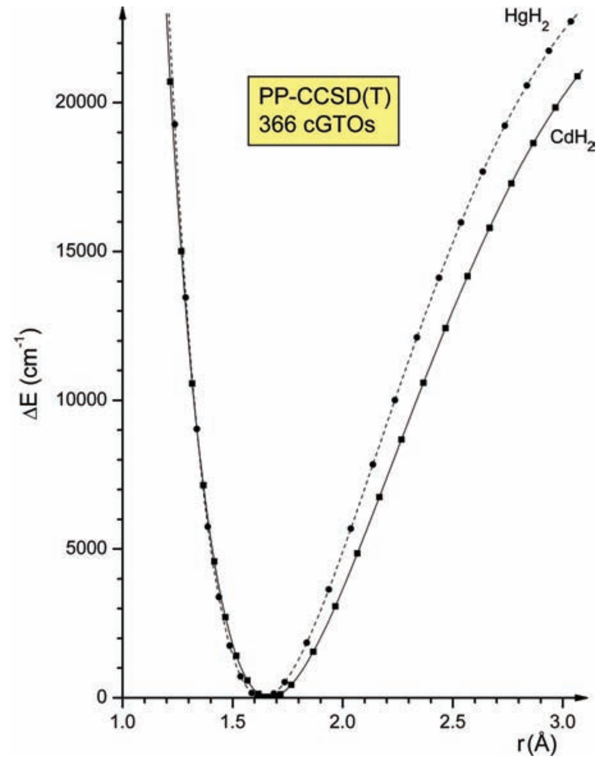

Figure 1. Variation of the PP-CCSD(T) energy with single metal−hydrogen bond distance for CdH_2 and HgH_2.

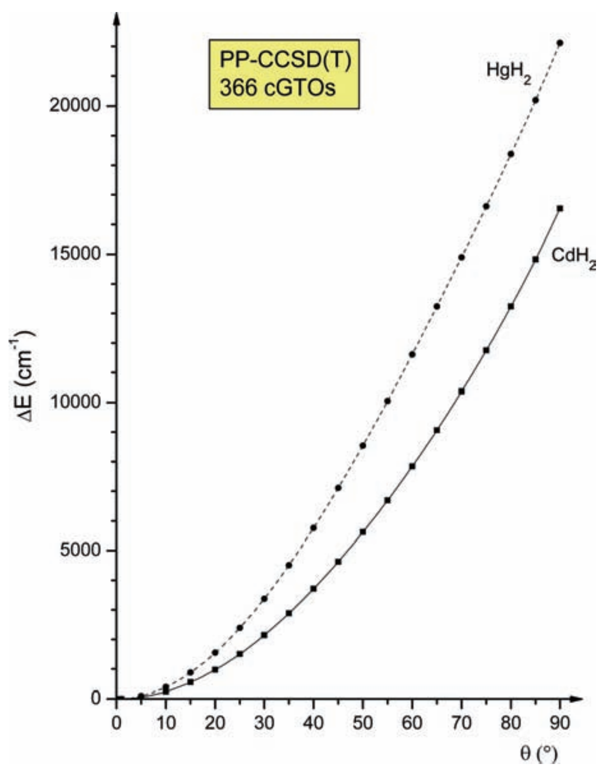

Figure 2. Variation of the PP-CCSD(T) energy with the change in the H−Me−H bond angle for CdH_2 and HgH_2.

The most important difference in the electronic structure of CdH_2 and HgH_2 appears to be the energetic shift of the highest occupied d shell. This shift is about 0.1 E_h, from −0.72 E_h for Cd 4d to −0.60 E_h for Hg 5d, in the case of the free atoms (SO-averaged values), and is partly due to relativistic effects. In the case of the dihydrides, the shift is quite similar to the atomic values, from −0.75 E_h to −0.65 E_h. Such a shift allows for significant bonding interaction with H 1s orbitals (at −0.5 E_h in the free atoms) in the case of HgH_2, thereby stabilizing the dσ level by 0.06 E_h with respect to the dπ and dδ levels. This bonding interaction adds to the sσ bond between the Hg 6s orbital and the hydrogen 1s orbitals. The corresponding splitting of the Cd d levels is ~0.01 E_h only; i.e., the dσ bonding contribution is small. The presence of a significant amount of directional dσ bonding in the case of HgH_2 may explain the steeper bending potential and is probably also responsible in part for the larger stretching force constant.

Two different analytical potential energy functions (PEFs) were established for CdH_2 in the present work, both of which have the following form:

$$V - V_e = \sum_{ijk} C_{ijk} \tilde{r}_1^i \tilde{r}_2^j \theta^k \quad (1)$$

In eq 1, the angle θ measures the deviation from linearity and $\tilde{r}$ is a dimensionless Morse-like coordinate[22] of the form

$$\tilde{r} = \{1 - \exp[-\beta(r - r_e)/r_e]\}/\beta \quad (2)$$

At first, an uncorrected analytical PP-CCSD(T) PEF was constructed on the basis of 263 symmetry-unique energy points that cover a range of up to ca. 15 000 cm^{-1} above equilibrium. After a crude optimization of the nonlinear parameter β (resulting value: 1.05; kept fixed from now on), an ansatz with 32 nonredundant linear terms C_{ijk} (see Table 1) was found to yield a faithful representation of the PP-CCSD(T) potential energy surface in the given energy regime. The standard deviation of the least-squares fit is 6.3×10^{-7} E_h or 0.14 cm^{-1}.

In a second step, the analytical PP-CCSD(T) PEF was improved by making use of two precise pieces of experimental information, namely the ground-state rotational constant B_{000} and the band origin of the antisymmetric stretching vibration ν_3, both for the most abundant isotopomer $^{114}CdH_2$. These two experimental data were employed in an iterative way to refine the equilibrium bond length and to determine a single scaling factor for the two equivalent diagonal stretch-only parts of the PP-CCSD(T) PEF. The resulting PEF is termed PP-CCSD(T) + corr; its parameters are listed in Table 1. Owing to the lack of suitable high-resolution spectroscopic data, no experimental information on any pure bending vibration could be employed. However, due to the increase of r_e by 0.003613 Å upon inclusion of the empirical corrections, the bending and stretch−bending parts of the PP-CCSD(T) PEF experience slight changes.

2.2. Electric Dipole Moment Function. To calculate absolute intensities of rovibrational transitions, either in absorption or in emission, the knowledge of an electric dipole moment function (EDMF), describing the variation of the electric dipole moment vector with the nuclear coordinates, is required. The EDMF of the present work is obtained from PP-CCSD(T) calculations with the 366 cGTO basis set. The correlation contributions to the electric dipole moment components were calculated as numerical derivatives of the CCSD(T) correlation energies with respect to a uniform electric field with components of ±0.0002 au. These were then added to the corresponding PP-Hartree−Fock values, computed as expectation values, to obtain the total dipole moments.

TABLE 1: Nonredundant Parameters of Analytical Potential Energy Functions for CdH_2[a]

i	j	k	PP-CCSD(T)[b]	PP-CCSD(T) + corr[c]
2	0	0	0.6410809	0.6401043
3	0	0	−0.8155368	−0.8159004
4	0	0	0.6059212	0.6053099
5	0	0	−0.4263379	−0.4284624
6	0	0	0.0770552	0.0776038
0	0	2	0.0371672	0.0369601
0	0	4	−0.0058344	−0.0057707
0	0	6	0.0017699	0.0017560
0	0	8	−0.0002661	−0.0002661
0	0	10	0.0000268	0.0000268
1	1	0	0.0161187	0.0152497
2	1	0	−0.1007855	−0.0997298
3	1	0	0.0807325	0.0789614
2	2	0	0.1248033	0.1227880
4	1	0	−0.1268251	−0.1276652
3	2	0	−0.1533401	−0.1549611
5	1	0	−0.0450125	−0.0450125
4	2	0	−0.0813097	−0.0813097
3	3	0	−0.1409232	−0.1409232
1	0	2	−0.0478651	−0.0476971
1	1	2	0.0684007	0.0685859
2	0	2	0.0044163	0.0046321
2	1	2	0.0219476	0.0207812
3	0	2	0.0254592	0.0256870
2	2	2	−0.0821228	−0.0821228
3	1	2	−0.1246668	−0.1246668
4	0	2	−0.0579195	−0.0579195
1	0	4	0.0147378	0.0146386
1	1	4	−0.0309825	−0.0309825
2	0	4	−0.0073423	−0.0074307
3	0	4	−0.0135999	−0.0135999
1	0	6	−0.0032132	−0.0032132

[a] Throughout, the nonlinear parameter β has a value of 1.05. The mathematical forms of the PEFs are described in eqs 1 and 2. [b] r_e = 1.666792 Å. [c] r_e = 1.670405 Å.

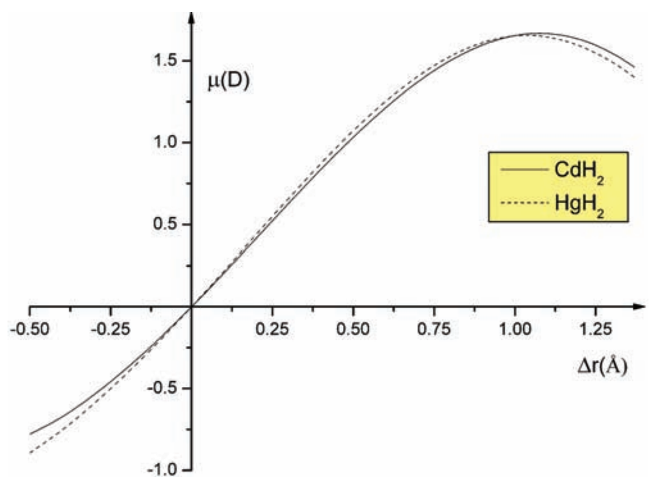

Figure 3. Electric dipole moment of CdH_2 and HgH_2 as a function of the change in the single metal−hydrogen bond distance.

The variation of the electric dipole moment for CdH_2 and HgH_2 with respect to single metal−hydrogen bond stretching is shown in Figure 3. The curves for CdH_2 and HgH_2 are rather similar, with slopes at equilibrium differing by less than 6% and maxima of similar heights at close locations. Much larger differences are observed when the molecules are bent (see Figure 4). The dipole moment curve for CdH_2 is much steeper and exhibits little curvature while that for

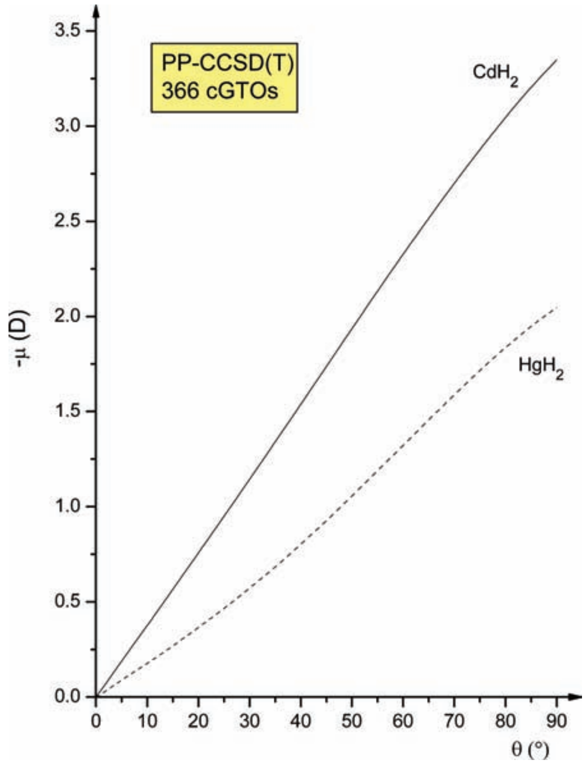

Figure 4. Dependence of electric dipole moment for CdH_2 and HgH_2 on the change of the H−Me−H bond angle.

HgH_2 displays almost S-shape behavior with a point of inflection close to $\theta = 60°$. The steeper slope for CdH_2 may be attributed to the fact that the ionization potential for the Cd atom is significantly smaller than for the Hg atom (8.99 vs 10.43 eV). Thus the Cd−H bond is expected to be more ionic than the Hg−H bond leading to a larger dipole moment for nonlinear geometries of CdH_2 compared to HgH_2.

The expansion of the EDMF was carried out around the minimum of the corrected potential energy surface. The originally calculated components of the dipole moment, termed μ_z and μ_x, were transformed to the molecular Eckart frame. Values for the resulting components, termed $\mu^{\parallel}$ and $\mu^{\perp}$, were obtained by a least-squares fit to the function

$$\mu_\alpha = \sum_{ijk} D_{ijk}{}^{\alpha} S_1{}^{i} S_3{}^{j} \theta^{k} \qquad (\alpha\text{: parallel or perpendicular}) \tag{3}$$

where S_1 and S_3 are symmetry coordinates, defined as $S_1 = 2^{-1/2}(r_1 + r_2 - 2r_e)$ and $S_3 = 2^{-1/2}(r_1 - r_2)$, respectively. The parallel component of the electric dipole moment is of σ_u symmetry, while the perpendicular component is of π_u symmetry. Consequently, the former is fitted with odd values of j and even values of k, whereas the latter component is fitted with even values of j and odd values of k. There are no restrictions on the index i. In total, dipole moments were calculated at 111 nuclear configurations and the two components were fitted with 18 and 23 terms, respectively. The EDMF parameters for $^{114}CdH_2$ are listed in Table 2. For other isotopomers, an appropriate transformation of the dipole moment components was carried out in the course of the calculation of dipole moment matrix elements over rovibrational basis functions.

TABLE 2: PP-CCSD(T) Electric Dipole Moment Function (EDMF) for CdH_2[a]

i	j	k	$D_{ijk}^{\parallel}$	i	j	k	$D_{ijk}^{\perp}$
0	1	0	0.59336	0	0	1	−0.84867
0	3	0	−0.01322	0	0	3	−0.05876
0	5	0	0.00198	0	0	5	0.03825
1	1	0	0.11368	0	0	7	−0.00612
1	3	0	−0.01207	1	0	1	−0.17870
1	5	0	0.00349	1	0	3	0.05553
2	1	0	−0.11598	1	0	5	−0.01374
2	3	0	−0.00630	2	0	1	0.04194
0	1	2	0.04029	2	0	3	0.00486
0	1	4	0.01662	2	0	5	0.00482
0	3	2	−0.01522	3	0	1	0.01154
0	3	4	0.00035	3	0	3	−0.00104
0	5	2	0.00131	4	0	1	0.00448
1	1	2	0.04833	0	2	1	0.05077
2	1	2	−0.08827	0	4	1	0.00113
1	1	4	−0.00642	0	2	3	0.00791
2	1	4	−0.00291	0	4	3	−0.00132
1	3	2	0.03249	0	2	5	−0.00144
				1	2	1	−0.00220
				2	2	1	0.02108
				1	2	3	0.01139
				3	2	1	−0.01139
				1	2	5	0.00781

[a] The EDMF is expanded around $r_e = 1.670405$ Å (minimum of corrected PEF). All EDMF terms (for definition see eq 3) are given in ea_0.

3. Rovibrational Term Energies and Spectroscopic Constants

3.1. Details of Calculations. The two PEFs from Table 1 were used in variational calculations of rovibrational term energies and wave functions. For this purpose, Watson's isomorphic rovibrational Hamiltonian for linear molecules[23] was diagonalized in a basis of harmonic oscillator/rigid rotor functions, using a program written by one of us.[24] Utilizing g/u-symmetry for the symmetrical isotopomers CdH_2 and CdD_2, a product basis of 451 vibrational functions yields the term energies of vibrational states up to $3\nu_3$ with a numerical accuracy of 0.01 cm^{-1} or better. In the calculations for CdHD, a basis set of 876 vibrational functions was employed to achieve comparable accuracy. The total size of the basis in the various calculations performed scales linearly with the rotational quantum number J.

Since the comparison of frequencies of individual rovibrational transitions is too extensive and mostly not very instructive, comparison between theory and experiment is commonly carried out at the stage of so-called spectroscopic constants. In the present work, these were obtained by a least-squares fit to the calculated rovibrational term energies. For levels with vibrational angular momentum quantum number $l = 0$, the fits were restricted to the first 11 levels ($J = 0-10$) and carried out by means of the well-known formula

$$E_v(J) = G_v + B_v[J(J+1)] - D_v[J(J+1)]^2 \tag{4}$$

Here, v stands for a triple of vibrational quantum numbers: v_1 for the symmetric stretching vibration, v_2 for the bending vibration, and v_3 for the antisymmetric stretching vibration. In eq 4, G_v denotes the vibrational term energy, B_v the rotational constant, and D_v the centrifugal distortion constant. For states with $l \neq 0$ l-type doubling and, if necessary, l-type rotational resonances have to be taken into account. This can be achieved by setting up an effective Hamiltonian matrix along the lines described by Nielsen and co-workers.[25−27] Its diagonal elements have the form

$$\langle v,J,l|H_{\mathrm{eff}}|\mathrm{v},J,l\rangle = G_{\mathrm{v}} + B_{\mathrm{v}}[J(J+1) - l^2] - D_{\mathrm{v}}[J(J+1) - l^2]^2 \quad (5)$$

The spectroscopic parameters G_v, B_v, and D_v now include contributions from vibrational angular momentum. E.g., G_v includes the additive term $g_{22}l^2$.

The off-diagonal elements are given by

$$\langle v,J,l|H_{\mathrm{eff}}|\mathrm{v},J,l \pm 2\rangle = 1/4[q_{\mathrm{v}} + q_{\mathrm{D}}(J+1)]\{[(v_2+1)^2 - (l \pm 1)^2][J(J+1) - l(l \pm 1)][J(J+1) - (l \pm 1)(l \pm 2)]\}^{1/2} \quad (6)$$

The rotational quantum number J must fulfill the relation $J \geq l$. For a given value of v_2, l may take $n = v_2 + 1$ different values: v_2, $v_2 - 2$, ..., $-v_2 - 2$, $-v_2$. Individual spectroscopic parameters were obtained through diagonalization of n x n effective Hamiltonian matrices in conjunction with least-squares fitting.

The calculated rovibrational wave functions together with the matrix elements of the EDMF were employed to calculate the squared transition dipole moments μ_{if}^2 between rovibrational states closely following the detailed description in ref 28. Together with appropriate statistical weight factors, the μ_{if}^2 values may be used to simulate infrared absorption spectra. The squared transition dipole moment may approximately be written as a product of three factors: $\mu_{\mathrm{if}}^2 \approx F_{\mathrm{HL}}F_{\mathrm{HW}}\mu_{\mathrm{vv'}}^2$, where F_{HL} is the Hönl−London factor, F_{HW} is the Herman−Wallis factor, and $\mu_{\mathrm{vv'}}$ is the transition dipole moment of the pure vibrational transition. For F_{HW} an expression of the form $[1 + A_1m + A_2m^2]^2$ was used with $m = -J$ and $m = J + 1$ for P-branch and R-branch transitions, respectively.[29] Integrated molar absorption intensities of fundamental rovibrational bands were then calculated by the well-known formula[30]

$$A_{\mathrm{f0}} = \frac{\pi N_{\mathrm{A}}}{3\hbar c_0 \varepsilon_0}\bar{\nu}_{f0}|\mu_{\mathrm{f0}}|^2 \quad (7)$$

Here, N_A is Avogadro's number, $\hbar$ is Planck's constant divided by 2π, c_0 is the vacuum velocity of light, ε_0 is the permittivity of vacuum, ν_{f0} is the vibrational wavenumber, and μ_{f0} is the corresponding vibrational dipole transition moment.

3.2. Results and Discussion. Calculated harmonic vibrational wavenumbers for $^{114}CdH_2$ and $^{114}CdD_2$ from earlier and the present work are compared in Table 3. Those obtained from PEF PP-CCSD(T) + corr (see last column of Table 3) are the most reliable ones, with estimated errors of only ca. 1 cm^{-1} in all six cases. Both for $^{114}CdH_2$ and for $^{114}CdD_2$, the difference $\omega_1 - \omega_3$ is small and thus indicative of Darling−Dennison resonance[31] at the first overtone level (see below). Interestingly, the difference is positive for $^{114}CdH_2$ while a sign change occurs upon deuteration. For ^{114}CdHD, the empirically corrected potential yields harmonic vibrational wavenumbers (in cm^{-1}) of 1843.4 (∼CH stretch), 546.6 (bend), and 1309.6 (∼CD stretch).

Before turning to the outcome of our variational calculations, it may be of interest to look at the results of calculations by means of standard second-order perturbation theory in normal coordinate space, nowadays often denoted by the acronym VPT2. Numerical techniques were employed to extract the necessary quartic force fields from the two PEFs described in Table 1. Results of the present calculations for $^{114}CdH_2$ and $^{114}CdD_2$ are given in Table 4 along with the corresponding values for $^{202}HgH_2$ and $^{202}HgD_2$, as calculated from PEF "PP/CCSD(T) + SO + corr" of ref 18. On the whole, the differences between the results obtained with the two PEFs used for CdH_2 are quite small and we will restrict the following discussion to the results obtained with the empirically corrected potential. Excellent agreement with experiment is observed for the l-type doubling constant q_2^e of $^{114}CdH_2$, $^{202}HgH_2$, and $^{202}HgD_2$, the differences amounting to 0.3, 0.4, and 0.9%, respectively. In accordance with the formula given by Watson,[32] the present q_2^e values have positive sign while Bernath and co-workers[4,6] used a different sign convention. Throughout, very good agreement between VPT2 values and experiment is also obtained for the vibration−rotation coupling constants of the two stretching vibrations, termed α_1 and α_3. The theoretical values for α_2 are larger than the corresponding experimental values, obtained as differences of rotational constants according to $\alpha_2 \approx B_{000} - B_{010}$, by 16% for $^{114}CdH_2$ and by 9−10% for the mercury dihydrides. The smaller deviations of the latter are related to the steeper bending potential in the case of HgH_2. In all cases, higher-order spectroscopic constants (γ_{ij}) would be required to accurately describe the v_2 dependence of the rotational constant in a perturbational treatment (see below for our variational results). All α_2 values have positive values which is rather unusual for linear molecules. As already mentioned in our earlier paper,[18] this is a common feature for the group 12 dihydrides (ZnH_2−HgH_2), however. An earlier example of a positive α_2 value was found in theoretical work for the cation $HOSi^+$.[33] In that paper, the individual contributions to α_2 were analyzed in detail. Interestingly, a sign change in α_2 was found upon deuteration.

TABLE 3: Calculated Harmonic Vibrational Wavenumbers (in cm^{-1}) for $^{114}CdH_2$ and $^{114}CdD_2$[a]

method and basis	ref[b]	$^{114}CdH_2$ ω_1	ω_2	ω_3	$^{114}CdD_2$ ω_1	ω_2	ω_3
PP-MP2/A[c]	8	1858	606	1844	1314	433	1316
PP-CCSD(T)/A[c]	8	1794	574	1790	1269	410	1278
PP-CCSD(T)/B[d]	8	1850	593	1829	1309	423	1305
B3LYP/6-311++G(3df, 3pd)	9	1825.8	646.6	1807.3	1291.5	461.3	1289.5
PP-CCSD(T)/366 cGTOs	*	1852.3	632.3	1845.3	1310.3	451.2	1316.6
PP-CCSD(T)+corr.	*	1846.3	629.2	1840.5	1306.0	448.9	1313.2

[a] According to common spectroscopic convention ω_1, ω_2, and ω_3 refer to symmetric stretching, bending, and antisymmetric stretching vibrations, respectively. [b] Results from the present work are marked with an asterisk. [c] cGTO basis: [6s, 5p, 3d / 2s, 1p]. [d] cGTO basis: [8s, 6p, 5d, 2f / 7s, 2p].

For centrosymmetric triatomic molecules the perturbational result for α_2 may be written as

$$\alpha_2 = \frac{q_2^{\mathrm{e}}}{2} + \alpha_2^{\mathrm{anh}} \tag{8}$$

with

$$\alpha_2^{\mathrm{anh}} = -2\pi B_{\mathrm{e}}^{\,2}\left(\frac{c}{h}\right)^{1/2}\phi_{122}\frac{a_1}{\omega_1^{\,3/2}} \tag{9}$$

In eq 9, ϕ_{122} is the cubic normal coordinate force constant involving the symmetric stretching and bending normal coordinate and a_1 is the derivative of the moment of inertia with respect to the totally symmetric normal coordinate, taken at equilibrium. For $^{114}CdH_2$ the anharmonic contributions to α_2 are calculated to be −0.01387 and −0.00495 cm^{-1}, while values of −0.00901 and −0.00321 cm^{-1} are obtained for $^{202}HgH_2$ and $^{202}HgD_2$, respectively.

Table 4 also allows for some comparison between theory and experiment for the anharmonicity constants X_{ij}. Excellent agreement is observed for X_{13} and X_{23}. The experimental values for X_{33} were not corrected for Darling−Dennison resonance, but the much smaller differences between calculated and experimental X_{33} values for $^{202}HgH_2$ and $^{202}HgD_2$ are a clear indication that this second-order anharmonic resonance plays a minor role for mercury dihydride.

The last line of Table 4 quotes calculated values for the spectroscopic constant g_{22}, which describes the contribution of the vibrational angular momentum to the vibrational energy. Throughout, the g_{22} values are significantly smaller than the corresponding equilibrium rotational constants B_{e}. This prediction has important consequences for the relative locations of the rotational levels of the (0,3^1,0) and (0,3^3,0) states, which in turn are responsible for the nature of the perturbations found experimentally for the (0,0^0,1)e rotational levels of $^{114}CdH_2$ (see below).

Vibrational term energies for $^{114}CdH_2$ and $^{114}CdD_2$ as obtained from variational calculations with the two analytical PEFs of the present work (see Table 1) are listed in Table 5. All vibrational states with 1 = 0 up to the second overtone of the antisymmetric stretching vibration (0,0^0,3) are included. Experimental values, available only for the singly excited state (0,0^0,1) of both isotopomers and for the corresponding first overtone of $^{114}CdH_2$, are given in parentheses. Calculations with the PP-CCSD(T) PEF overestimate the term energies of the (0,0^0,1) and (0,0^0,2) states of $^{114}CdH_2$ by 4.8 and 12.7 cm^{-1}, respectively, while the deviation from experiment for the (0,0^0,1) state of $^{114}CdD_2$ amounts to 3.1 cm^{-1}. The corrected empirically PEF underestimates the latter value by only 0.3 cm^{-1} and overestimates the term energy of the (0,0^0,2) state of $^{114}CdH_2$ by 2.0 cm^{-1}. Actually, this state is more precisely described as the upper component of a Darling−Dennison resonance between states (2,0^0,0) and (0,0^0,2). While the singly excited stretching vibrational states of $^{114}CdH_2$ are separated by only 3.0 cm^{-1}, with the antisymmetric stretching vibration lying lower, anharmonic interaction at the first overtone level results in a rather large gap of 51.4 cm^{-1}. The corresponding data for $^{114}CdD_2$ are −8.0 and 32.0 cm^{-1}, respectively. As expected and as we will see later, the interaction between the two Darling−Dennison resonance components is almost independent of the total rotational quantum number J. On the whole, the corrected PEF should deliver quite accurate predictions for all the other vibrational states considered in Table 5. In particular, the (1,0^0,0) term values for $^{114}CdH_2$ and $^{114}CdD_2$ of 1774.5 and 1270.0 cm^{-1}, respectively, are expected to be in error by less than 1 cm^{-1}.

As noted by Bernath and co-workers,[6] the anharmonic interaction between vibrational levels (0,0^0,2) and (2,0^0,0) makes the isotopic splitting of lines from the (0,0^0,2)−(0,0^0,1) band very small. Actually, we may well use the isotopic shifts for the term energies of the relevant vibrational states as spectroscopic indicators of Darling−Dennison resonance. Table 6 quotes calculated and experimental shifts for all relevant stretching vibrational states of each five symmetric H and D isotopomers with respect to the most abundant species $^{114}CdH_2$ and $^{114}CdD_2$, respectively. Excellent agreement with experiment (largest difference: 0.003 cm^{-1}) is observed for the shifts in the ν_3 fundamentals. As expected, the shifts in the ν_1 wavenumbers are tiny; these would be exactly zero within the harmonic approximation. The shifts in the combination tones (1,0^0,1) differ only slightly (by less than 0.010 cm^{-1}) from the sum of the shifts in the (0,0^0,1) and (1,0^0,0) states. For the H isotopomers, the shifts in the vibrational term energies of the two components of the Darling−Dennison resonance are very similar, the largest difference amounting to 0.035 cm^{-1} for

TABLE 4: Spectroscopic Constants (in cm^{-1}) for $^{114}CdH_2$, $^{202}HgH_2$ and Their Dideuterated Species As Obtained by Second-Order Vibrational Perturbation Theory (VPT2)[a]

	$^{114}CdH_2$		$^{114}CdD_2$		$^{202}HgH_2$	$^{202}HgD_2$
constant	A[b]	B[c]	A[b]	B[c]		
B_{e}	3.01035	2.99735	1.50634	1.49983	3.13468 (3.13553)	1.56855 (1.56904)
$D_{\mathrm{e}}/10^{-5}$	3.180	3.160	0.796	0.791	2.778 (2.76)	0.696 (0.694)
q_2^{e}	0.04392	0.04367 (0.04380)	0.01541	0.01533	0.04360 (0.04342)	0.01536 (0.01522)
$q_2^J/10^{-6}$	−1.496	−1.486	−0.261	−0.259	−1.064	−0.186
α_1	0.04290	0.04273	0.01519	0.01513	0.04646 (0.04789)	0.01645 (0.01687)
α_2	0.00807	0.00797 (0.00688)	0.00275	0.00271	0.01279 (0.01161)	0.00447 (0.00412)
α_3	0.03240	0.03237 (0.03289)	0.01178	0.01177 (0.01191)	0.02813 (0.02983)	0.01014 (0.01064)
X_{11}	−16.05	−16.03	−8.03	−8.02	−21.07	−10.54
X_{12}	−10.56	−10.50	−5.27	−5.23	−16.14	−8.08
X_{13}	−59.34	−59.24	−29.81	−29.76	−70.95 (−70.79)	−35.57 (−35.67)
X_{22}	−4.77	−4.73	−2.44	−2.42	−6.30	−3.19
X_{23}	−13.41	−13.37 (−12.97)	−6.91	−6.89	−16.13 (−16.14)	−8.19 (−8.20)
X_{33}	−13.23	−13.25 (−1.26)[d]	−6.80	−6.81	−11.97 (−15.12)[d]	−6.10 (−7.34)[d]
g_{22}	2.03	2.02	1.05	1.04	2.46	1.25

[a] Experimental values (refs 4 and 6) are given in parentheses; the sign of q_2^{e} has been adjusted to the convention of the present paper. [b] PP-CCSD(T). [c] PP-CCSD(T)+corr. [d] Not corrected for Darling−Dennison resonance.

TABLE 5: Term Energies (in cm^{-1}) of 22 Lowest Excited Vibrational States ($l = 0$) for $^{114}CdH_2$ and $^{114}CdD_2$[a]

	$^{114}CdH_2$		$^{114}CdD_2$	
(v_1, v_2, v_3)	PP-CCSD(T)	PP-CCSD(T) + corr	PP-CCSD(T)	PP-CCSD(T) + corr
(0,2,0)	1205.4	1199.5	871.7	867.4
(0,0,1)	1776.3	1771.5 (1771.5)	1281.4	1278.0 (1278.3)
(1,0,0)	1780.4	1774.5	1274.2	1270.0
(0,4,0)	2378.4	2366.9	1726.0	1717.6
(0,2,1)	2956.2	2945.6	2139.8	2132.1
(1,2,0)	2965.4	2953.7	2135.7	2127.3
(1,0,1)	3498.4	3487.8	2526.2	2518.6
(2,0,0)	3501.7	3491.1	2525.2	2517.2
(0,6,0)	3522.1	3505.2	2564.0	2551.7
(0,0,2)	3553.2	3542.5 (3540.5)	2556.4	2549.2
(0,4,1)	4104.6	4088.5	2981.1	2969.4
(1,4,0)	4118.4	4101.2	2979.9	2967.5
(0,8,0)	4639.5	4617.5	3387.0	3370.8
(1,2,1)	4658.0	4641.6	3374.4	3362.6
(2,2,0)	4660.5	4644.3	3374.8	3362.7
(0,2,2)	4713.7	4697.0	3403.2	3391.7
(2,0,1)	5165.3	5149.2	3746.1	3734.6
(1,0,2)	5165.8	5149.8	3746.5	3734.9
(0,6,1)	5224.7	5203.2	3806.5	3790.9
(1,6,0)	5242.4	5219.9	3808.1	3791.7
(3,0,0)	5269.5	5252.3	3792.7	3780.8
(0,0,3)	5273.0	5258.2	3812.4	3802.0
ZPE[b]	2446.6	2438.1	1747.0	1741.0

[a] Experimental values (ref 6) in parentheses. [b] Zero-point vibrational energy.

TABLE 6: Isotopic Shifts (in cm^{-1}) in Term Energies of Lowest Stretching Vibrational States[a]

	$(0,0^0,1)$		$(1,0^0,0)$	$(2,0^0,0)$	$(1,0^0,1)$	$(0,0^0,2)$	
isotopomer	theor	exp	theor	theor	theor	theor	exp
$^{110}CdH_2$	0.538	0.538	−0.003	0.504	0.525	0.539	0.577
$^{111}CdH_2$	0.399	0.400	−0.002	0.375	0.390	0.399	0.430
$^{112}CdH_2$	0.264	0.265	−0.002	0.249	0.258	0.263	0.283
$^{113}CdH_2$	0.131	0.131	−0.001	0.123	0.128	0.130	0.141
$^{116}CdH_2$	−0.255	−0.256	0.001	−0.243	−0.249	−0.252	−0.270
$^{110}CdD_2$	0.771	0.771	−0.003	0.295	0.759	1.215	
$^{111}CdD_2$	0.573	0.573	−0.002	0.221	0.564	0.901	
$^{112}CdD_2$	0.379	0.378	−0.001	0.148	0.373	0.594	
$^{113}CdD_2$	0.188	0.187	−0.001	0.074	0.184	0.293	
$^{116}CdD_2$	−0.366	−0.369	0.001	−0.148	−0.360	−0.569	

[a] Shifts are quoted with respect to $^{114}CdH_2$ or $^{114}CdD_2$. Theoretical values refer to calculations with PEF PP-CCSD(T) + corr, which make use of the experimental value for ν_3($^{114}CdH_2$).

$^{110}CdH_2$. Likewise, the experimental and theoretical values for the shift ratio $(0,0^0,2)/(0,0^0,1)$ are rather close to unity. Actually, the magnitude of the resonance interaction appears to be slightly overestimated in our theoretical treatment. For the deuterated species, the present calculations predict significantly weaker anharmonic interaction, with shift ratios lying in the range 1.55−1.58.

No gas-phase high-resolution spectroscopic studies have yet been published for $^{114}CdHD$, so the theoretical values collected in Table 7 stand as predictions. The band origins of the two IR active stretching vibrations, as obtained from the corrected PEF at ν_1 = 1773.9 cm^{-1} (∼CdH stretch) and ν_3 = 1273.3 cm^{-1} (∼CdD stretch), should be in error by no more 1 cm^{-1}. The corresponding experimental values from argon matrix IR spectroscopy are 1756.9 and 1260.8 cm^{-1}.[8] The differences between matrix data and the present predictions amount to 17.0 and 12.5 cm^{-1} and are thus very close to the differences between experimental gas-phase values[6] and argon matrix values[8] for the ν_3 bands of $^{114}CdH_2$ and $^{114}CdD_2$ (18.0 and 13.4 cm^{-1}, respectively).

Rotational constants B_v and quartic centrifugal distortion constants D_v for $^{114}CdH_2$ and $^{114}CdD_2$ are collected in Table 8 for the vibrational ground state and pure stretching vibrational states up to $(0,0^0,3)$; the corrected PEF was used to arrive at the calculated data. The change in the rotational constant with excitation of the antisymmetric stretching vibration by one or two vibrational quanta is reproduced very well by the present calculations. Theory yields reductions by 0.03268 and 0.07526 cm^{-1}; the corresponding experimental values are 0.03289 and 0.07509 cm^{-1}, respectively. While the rotational constants of the singly excited stretching vibrational states $(1,0^0,0)$ and $(0,0^0,1)$ of $^{114}CdH_2$ differ by 0.01033 cm^{-1}, those for the corresponding first overtones show a difference of only 0.00135 cm^{-1}, which may be considered as a spectroscopic signature of strong Darling−Dennison resonance. Excellent agreement with experiment is obtained for B_{000} ($^{114}CdD_2$) and B_{001} ($^{114}CdD_2$), deviations not exceeding 0.0009 cm^{-1}. For the vibrationally excited states, the calculated D_v values are almost within experimental uncertainties.

Table 9 deals with theoretical and experimental spectroscopic parameters for the lowest bending vibrational states of $^{114}CdH_2$ and $^{114}CdD_2$. Besides the results from our variational calculations it includes G_v values, as calculated from the data of Table 4. For the lowest bending vibrational state $(0,1^1,0)$ agreement

TABLE 7: Calculated Vibrational Term Energies (l = 0) for ^{114}CdHD (in cm^{-1})

(v_1,v_2, v_3)[a]	PP-CCSD(T)	PP-CCSD(T) + corr
(0,2,0)	1053.0	1047.9
(0,0,1)	1277.1	1273.3
(1,0,0)	1779.2	1773.9
(0,4,0)	2080.6	2070.5
(0,2,1)	2317.7	2308.8
(0,0,2)	2525.6	2518.0
(1,2,0)	2810.1	2799.7
(1,0,1)	3053.9	3044.7
(0,6,0)	3084.7	3069.9
(0,4,1)	3332.8	3319.0
(2,0,0)	3501.9	3491.3
(0,2,2)	3553.7	3541.0
(0,0,3)	3745.7	3734.3
(1,4,0)	3816.2	3800.9
(0,8,0)	4067.7	4048.3
(1,2,1)	4072.4	4058.2
(1,0,2)	4299.8	4286.8
(0,6,1)	4324.9	4306.4
(2,2,0)	4510.6	4495.0
(0,4,2)	4556.5	4539.0
(0,2,3)	4761.2	4744.8
(2,0,1)	4773.9	4759.5
(1,6,0)	4799.5	4779.5
(0,0,4)	4937.4	4922.2
(0,10,0)	5031.4	5007.6
(1,4,1)	5066.2	5047.2
(3,0,0)	5168.5	5152.6
ZPE[b]	2104.3	2097.0

[a] Quantum numbers v_1, v_2, and v_3 correspond to CdH stretch, bend, and CdD stretch, respectively. [b] Zero-point vibrational energy.

between VPT2 results and variational theory is excellent, differences not exceeding 1 cm^{-1}. While the performance of VPT2 continues to be very good for the higher excited bending vibrational states of ^{114}CdD$_2$, differences of up to 6.0 cm^{-1} are observed for ^{114}CdH$_2$. The G_v values or band origins of the ν_2 bands of ^{114}CdH$_2$ and ^{114}CdD$_2$ are predicted to be 605.9 and 436.9 cm^{-1}, respectively. While no high-resolution gas-phase values are yet available, Wang and Andrews[9] have published ν_2 values referring to inert media such as solid neon and solid H$_2$ or D$_2$. These are in the range 603.7−605.1 cm^{-1} for CdH$_2$ and 434.3−435.6 cm^{-1} for CdD$_2$. The corresponding data for less inert solid argon are 601.7 and 432.5 cm^{-1},[8] respectively. On the basis of the comparison with the experimental results, we are confident that our calculated values are within ca. 1 cm^{-1} of the still unknown gas-phase data. For asymmetrically substituted ^{114}CdHD a value of 529.0 cm^{-1} is predicted. From the emission experiments,[6] precise gas-phase data are available for four spectroscopic constants (B, D, q_v, and q_D) of ^{114}CdH$_2$. Throughout, excellent agreement with the theoretical values is observed. The difference of rotational constants $B_{000}-B_{010}$ is calculated to be 0.00678 cm^{-1}, only 1.4% off from the experimental value.

As mentioned earlier, a major item of the present study concerns the perturbations observed in the emission spectra. For this purpose, we graphically investigate the dependence of the relevant series of rovibrational term energies with the rotational quantum number J. At the lowest possible J values, l is a reasonably good quantum number for the assignment process. Increasing the J value by unity, there is mostly only a slight change in the vibrational part of the rovibrational wave function and we may thus use an overlap criterion for the assignment of neighbored rovibrational states. In a few cases of accidental resonances, however, this criterion turned out to be not sufficient and so, as a second criterion, the smooth variation of the average l value was taken into account, as well. In the figures to follow (Figures 5−8), the relative energies of rovibrational states within an assigned series are connected by polygons, such that crossings may occur between different series.

We are now ready for a closer look at the perturbations found experimentally in the (0,0^0,1) state at J values between 12 and 17. From an energetic point of view and parity requirements, the e parity levels of states (0,3^1,0) (Π_u) and (0,3^3,0) (Φ_u) are the only possibilities. Table 10 quotes the calculated rovibrational term energies of the three states under consideration up to J = 30; for completeness, the f levels are included as well. According to perturbation theory, the G_v value of the (0,3^3,0) state lies above the (0,3^1,0) state by 8g_{22} or 16.1 cm^{-1}. Owing to the condition $J \geq l$ and since the rotational constant is larger than g_{22} (see Table 4), all of the allowed (0,3^3,0)e levels come to lie below the corresponding (0,3^1,0)e levels. This situation is shown in Figure 5, which draws the two sorts of levels relative to the corresponding (0,0^0,1) levels. The latter are crossed by the (0,3^3,0)e levels between J = 14 and J = 15, in excellent agreement with the emission spectra.[6] The spectra show "that the perturbation pushes the 001 ($^1\Sigma_u^+$) state J = 12−14 levels to lower energy, and pushes the J = 15−17 levels to higher energy",[6] which is exactly what we calculate.

As is shown in Figure 6, the perturbations observed for the (0,1^1,1)e levels at J = 9−13 are predicted to arise through interaction with (0,4^2,0)e levels. The minimum separation is calculated at J = 10 and amounts to 0.32 cm^{-1}. For J = 11 a value of 0.34 cm^{-1} is found. To get a deeper understanding of the perturbation, (0,1^1,1)e,f and (0,4^{0,2,4},0)e,f levels were fitted

TABLE 8: Rotational and Centrifugal Distortion Constants (in cm^{-1}) for Stretching Vibrational States (l = 0) of ^{114}CdH$_2$ and ^{114}CdD$_2$ (PP-CCSD(T) + corr)[a]

	^{114}CdH$_2$		^{114}CdD$_2$	
(v_1, v_2, v_3)	B_v	D_v/10^{-5}	B_v	D_v/10^{-5}
(0,0,0)	2.95254 (2.95254)	3.191 (3.179)	1.48385 (1.48421)	0.796 (0.797)
(0,0,1)	2.91986 (2.91964)	3.208 (3.194)	1.47202 (1.47229)	0.798 (0.796)
(1,0,0)	2.90953	3.174	1.46868	0.793
(1,0,1)	2.87644	3.194	1.45675	0.796
(2,0,0)	2.87593	3.390	1.45477	0.813
(0,0,2)	2.87728 (2.87745)	2.987 (2.996)	1.45882	0.773
(2,0,1)	2.83615	3.254	1.44213	0.801
(1,0,2)	2.83688	3.285	1.44178	0.817
(3,0,0)	2.82924	3.079	1.44126	0.769
(0,0,3)	2.84977	3.139	1.44741	0.846

[a] Experimental values (ref 6) are given in parentheses. The calculated B_v and D_v values result from fits with eq 4 considering J values up to 10.

TABLE 9: Theoretical and Experimental Spectroscopic Constants (in cm^{-1}) for the Lowest Bending Vibrational States of $^{114}CdH_2$ and $^{114}CdD_2$[a]

isotopomer	state		G_v[b]	g_{22}	B_v	$D_v/10^{-5}$	$q_v/10^{-2}$	$q_D/10^{-6}$
$^{114}CdH_2$	$(0,1^1,0)$	theor[a]	605.9 (605.1)		2.94576	3.235	4.377	−1.59
		exp[c]			2.94566	3.222	4.380	−1.69
	$(0,2^0,0)$	theor[a]	1199.5 (1196.7)	1.866	2.94049	3.293	4.399	−1.65
	$(0,2^2,0)$	theor[a]	1207.0 (1204.8)		2.93933	3.282		
	$(0,3^1,0)$	theor[a]	1788.9 (1782.9)	1.829	2.93553	3.351	4.423	−1.73
	$(0,3^3,0)$	theor[a]	1803.5 (1799.0)		2.93324	3.336		
$^{114}CdD_2$	$(0,1^1,0)$	theor[a]	436.9 (436.7)		1.48145	0.804	1.535	−0.27
	$(0,2^0,0)$	theor[a]	867.4 (866.4)	0.982	1.47943	0.814	1.541	−0.28
	$(0,2^2,0)$	theor[a]	871.4 (870.6)		1.47913	0.813		
	$(0,3^1,0)$	theor[a]	1295.6 (1293.4)	0.969	1.47750	0.824	1.547	−0.28
	$(0,3^3,0)$	theor[a]	1303.3 (1301.7)		1.47690	0.821		

[a] From variational calculations with the empirically corrected PEF. See section 3.1 for the determination of the spectroscopic constants; *J* values up to 10 were considered in the least-squares fits. For the definition of *l*-type doubling constants see ref 34. [b] VPT2 values are given in parentheses. All G_v values include *l*-dependent contributions. [c] Reference 6.

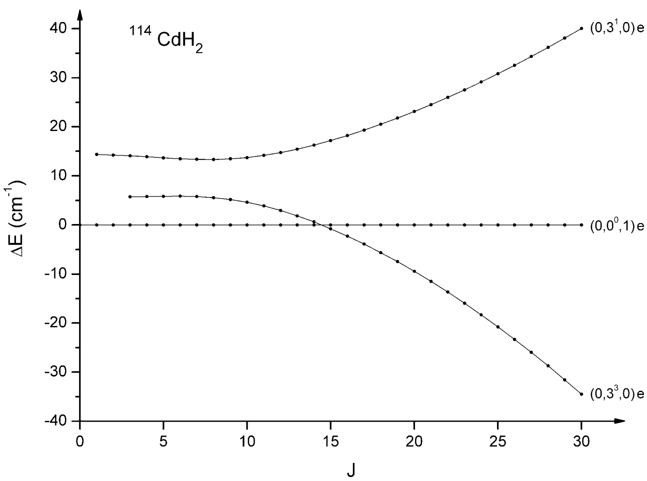

Figure 5. Relative energies of e parity levels for $(0,3^1,0)$ and $(0,3^3,0)$ states of $^{114}CdH_2$, taken with respect to $(0,0^0,1)$e levels.

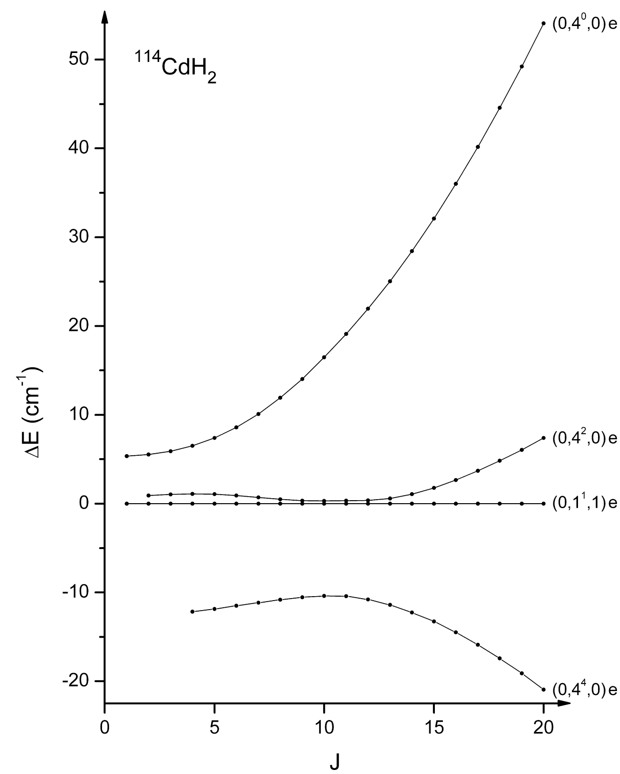

Figure 6. Relative energies of e parity levels for $(0,4^l,0)$ states ($l = 0$, 2, 4) states of $^{114}CdH_2$, taken with respect to $(0,1^1,1)$e levels.

according to eqs 5 and 6 over a range of $J = 0$ up to $J = 30$, without taking the perturbed states ($J = 5-17$) into account. The obtained spectroscopic constants were then used to calculate the energy difference between the two resonating states also for values of *J* for which a perturbation was found. In this way, significantly smaller differences of 0.06 and 0.02 cm^{-1} were found for $J = 10$ and 11, respectively. Apparently, we have to deal with a slight, rather local perturbation.

While no perturbations were found in the emission spectra of deuterated species,[6] the present calculations identified a number of perturbations of which the one with lowest energy is shown in Figure 7. Here, $(0,4^4,0)$e levels interact with $(0,1^1,1)$e levels, with a crossing point almost exactly at $J = 21$.

Finally, Figure 8 shows the complex system of levels interacting in the region of the Darling−Dennison resonance system. As expected, the relative energies of the $(2,0^0,0)$ levels depend only slightly on *J*, the level separation with respect to $(0,0^0,2)$ levels amounting to 51.427 cm^{-1} at $J = 0$ and to 55.852 cm^{-1} at $J = 30$. The rather small difference of 4 cm^{-1} may be compared with an increase in rotational energy in the $(0,0^0,2)$ state of as much as 2650 cm^{-1}. According to the present calculations, $(0,0^0,2)$e levels are perturbed by $(0,6^0,0)$e near $J = 15$, which is in accord with the Supporting Information of ref 6. Further crossings are predicted between $(0,3^1,1)$e, $(0,6^2,0)$e, and $(0,0^0,2)$e levels for *J* values of between 25 and 29.

Calculated transition dipole moments and molar absorption intensities for several transitions of $^{114}CdH_2$, $^{114}CdD_2$, and $^{114}CdHD$ are given in Table 11. The largest intensity is calculated for the antisymmetric stretching vibration of $^{114}CdH_2$. The present value is smaller than the corresponding result for $^{202}HgH_2$[18] by 8%, in agreement with the slightly steeper dipole moment curve for the latter shown in Figure 3. On the other hand, the bending fundamental of $^{114}CdH_2$ is more intense than the corresponding band of $^{202}HgH_2$ by a factor of 4.2, reflecting the much steeper increase of the dipole moment with increasing deviation from linearity in the case of CdH_2 (see Figure 4). For all fundamentals of the CdH_2 isotopomers considered in Table 11, the double harmonic (DH) approximation performs quite well, as was the case for the corresponding mercury species.[18] As expected for a case of strong Darling−Dennison resonance, the transition dipole moments for transitions between the singly excited $(0,0^0,1)$ state and the two resonance components at the first overtone level are practically equal for $^{114}CdH_2$. On the other hand, about a factor of 2 difference is predicted for $^{114}CdD_2$, clearly indicating a less pronounced anharmonic interaction.

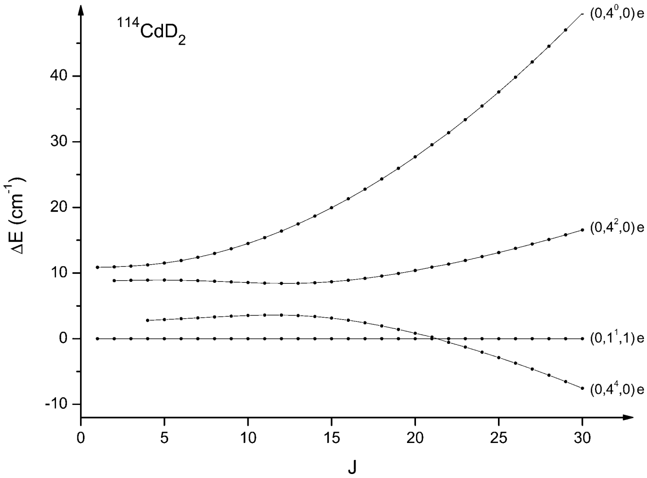

Figure 7. Relative energies of e parity levels for $(0,4^l,0)$ states ($l = 0$, 2, 4) states of $^{114}CdD_2$, taken with respect to $(0,1^1,1)$e levels.

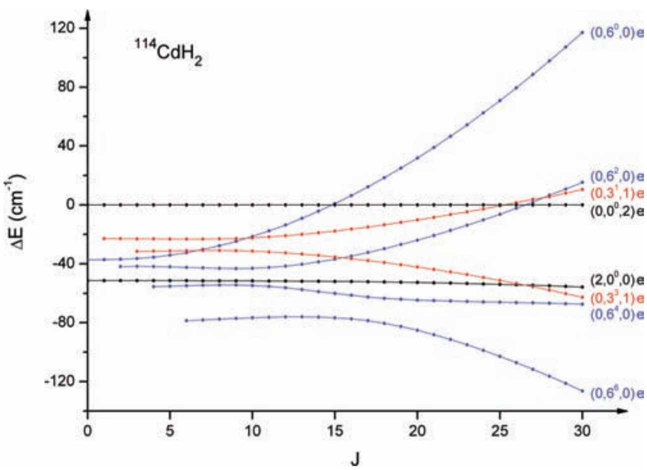

Figure 8. Relative energies of e parity levels of interacting states for $^{114}CdH_2$, which lie in the range of the Darling−Dennison resonance system between $(2,0^0,0)$ and $(0,0^0,2)$, the latter defining the energy zero of the figure.

The knowledge of Einstein coefficients of spontaneous emission is required to quantitatively interpret the intensities of emission spectra. Table 12 compares calculated values for a number of vibrational transitions in $^{114}CdH_2$, $^{202}HgH_2$ and their dideuterated species. Again, the effect of strong Darling−Dennison resonance is clearly discernible in the data for $^{114}CdH_2$. In particular, the Einstein coefficients for the three transitions $(0,0^0,2) \rightarrow (0,0^0,1)$, $(2,0^0,0) \rightarrow (0,0^0,1)$ and $(0,0^0,1) \rightarrow (0,0^0,0)$ are very similar for this molecule, while great differences apply for the other three species.

Like in our previous work on HgH_2 isotopomers, gas-phase IR spectra have been calculated for $^{114}CdH_2$, $^{114}CdD_2$, and $^{114}CdHD$. Since cadmium dihydride is only metastable, the dissociation process into Cd (^1S) + $H_2(X^1\Sigma_g^+)$ being exothermic, it will be very difficult to observe such spectra in the gaseous phase. Five figures with spectra for the infrared active bands of the three isotopomers are provided as Supporting Information.

4. Conclusions

Making use of a small-core energy-consistent pseudopotential for the cadmium atom[11] and a large basis set comprising 366 contracted Gaussian-type orbitals,[12−14] the near-equilibrium potential energy surface of CdH_2 ($X\ ^1\Sigma_g^+$) as well as its electric dipole moment surface were calculated at the CCSD(T) level of theory. An improved analytical PEF was obtained through the use of accurate experimental values for the ground-state rotational constant B_0 of the most abundant isotopomer $^{114}CdH_2$ and the corresponding wavenumber for the antisymmetric stretching vibration ν_3.[6] The equilibrium distance of CdH_2 is predicted to be $r_e = 1.6704$ Å, which may be compared with our previous recommended value for HgH_2 of 1.6332(1) Å[18] and an experimental r_e value for $^{64}ZnH_2$ of 1.5241 Å.[4] The bending potential of CdH_2 is significantly more shallow than that of HgH_2 and gives rise to a rather low-lying bending vibration, predicted to have its band origin at 605.9 cm^{-1}. The corresponding value for $^{202}HgH_2$ from our previous work[18] is $\nu_2 = 684.1$ cm^{-1}, higher by as much as 13%. While the two stretching vibrational wavenumbers of $^{202}HgH_2$ are separated by $\nu_3 - \nu_1 = 99.5$ cm^{-1}, the corresponding difference predicted

TABLE 10: Rovibrational Levels (in cm^{-1}) for $^{114}CdH_2$[a]

J	$(0,0^0,1)$e	$(0,3^1,0)$e	$(0,3^1,0)$f	$(0,3^3,0)$e	$(0,3^3,0)$f
0	1771.530				
1	1777.369	1791.716	1791.893		
2	1789.048	1803.281	1803.811		
3	1806.563	1820.636	1821.696	1812.290	1812.292
4	1829.914	1843.794	1845.554	1835.717	1835.725
5	1859.097	1872.774	1875.392	1864.957	1864.989
6	1894.107	1907.602	1911.217	1899.975	1900.070
7	1934.941	1948.313	1953.030	1940.728	1940.954
8	1981.593	1994.942	2000.831	1987.169	1987.631
9	2034.057	2047.520	2054.617	2039.254	2040.091
10	2092.326	2106.060	2114.381	2096.958	2098.326
11	2156.393	2170.555	2180.114	2160.272	2162.328
12	2226.247	2240.985	2251.807	2229.197	2232.089
13	2301.881	2317.326	2329.447	2303.740	2307.602
14	2383.277	2399.554	2413.022	2383.912	2388.858
15	2470.465	2487.645	2502.519	2469.675	2475.846
16	2563.370	2581.577	2597.923	2561.090	2568.558
17	2662.015	2681.333	2699.221	2658.115	2666.980
18	2766.384	2786.892	2806.395	2760.747	2771.102
19	2876.461	2898.237	2919.431	2868.977	2880.911
20	2992.233	3015.349	3038.310	2982.794	2996.392
21	3113.685	3138.211	3163.017	3102.186	3117.530
22	3240.799	3266.804	3293.531	3227.138	3244.310
23	3373.560	3401.109	3429.836	3357.635	3376.716
24	3511.949	3541.107	3571.909	3493.663	3514.730
25	3655.950	3686.777	3719.732	3635.203	3658.334
26	3805.542	3838.099	3873.283	3782.238	3807.510
27	3960.707	3995.052	4032.540	3934.750	3962.237
28	4121.424	4157.615	4197.480	4092.720	4122.495
29	4287.672	4325.763	4368.080	4256.126	4288.264
30	4459.429	4499.475	4544.316	4424.950	4459.521

[a] From variational calculations with PEF PP-CCSD(T) + corr.

TABLE 11: Transition Dipole Moments μ (in D) and Integrated Molar Absorption Intensities A (in km mol^{-1}) for $^{114}CdH_2$, $^{114}CdD_2$, and $^{114}CdHD$[a]

transition		$^{114}CdH_2$	$^{114}CdD_2$	$^{114}CdHD$
$10^00 \leftarrow 00^00$	μ	0^c	0^c	0.164
	A^b	0^c	0^c	86.4 (87.8)
$01^10 \leftarrow 00^00$	μ	0.435	0.366	0.405
	A^b	286.8 (284.6)	146.1 (144.9)	217.4 (214.8)
$00^01 \leftarrow 00^00$	μ	0.282	0.234	0.196
	A^b	356.3 (346.6)	175.8 (176.4)	183.4 (173.7)
$00^02 \leftarrow 00^01$	μ	0.283	0.295	0.280
$20^00 \leftarrow 00^01$	μ	0.285	0.154	0.001
$20^00 \leftarrow 10^00$	μ	0^c	0^c	0.234
$01^11 \leftarrow 01^10$	μ	0.287	0.234	0.196

[a] Calculated by means of PEF PP-CCSD(T) + corr and the EDMF of Table 2. [b] Double harmonic values are given in parentheses. [c] Zero by symmetry.

TABLE 12: Einstein Coefficients of Spontaneous Emission (in s^{-1}) for Vibrational Transitions of CdH_2 and HgH_2 Isotopomers[a]

transition	$^{114}CdH_2$	$^{114}CdD_2$	$^{202}HgH_2$	$^{202}HgD_2$
$(0,0^0,3) \rightarrow (0,0^0,2)$	158	88	430	125
$(0,0^0,3) \rightarrow (2,0^0,0)$	83	7	3	0
$(0,0^0,2) \rightarrow (0,0^0,1)$	140	56	334	90
$(2,0^0,0) \rightarrow (0,0^0,1)$	129	14	11	2
$(1,0^0,1) \rightarrow (1,0^0,0)$	128	34	162	44
$(0,0^0,1) \rightarrow (0,0^0,0)$	139	36	177	46
$(0,1^1,1) \rightarrow (0,1^1,0)$	140	35	175	46

[a] Based on calculations with the empirically corrected PEFs.

for $^{114}CdH_2$ in the present work is as low as -3.0 cm^{-1}; note that a change in the order of the two vibrations has occurred. Upon deuteration, the antisymmetric stretching vibration comes to lie above the symmetric stretching vibration and the difference in wavenumbers increases to 8.0 cm^{-1}. Owing to the small value of ν_3-ν_1 for $^{114}CdH_2$, pronounced Darling−Dennison resonance is predicted for the first overtone level, the calculated difference $2\nu_3 - 2\nu_1$ amounting to 51.4 cm^{-1}. It is only slightly smaller than the experimental value of 59.3 cm^{-1} as published for $^{64}ZnH_2$ by Shayesteh et al.[4]

Quantum-chemical calculations may play a very important role in the elucidation of perturbations observed in high-resolution spectra of small molecules, CdH_2 being a nice example of this sort. In contrast to the previous assignment proposed for the perturbations arising in the ν_3 band of $^{114}CdH_2$ (and other H isotopomers),[6] we have identified the $(0,3^3,0)$ state to be responsible for this issue. According to the calculations of the present work, the perturbations observed for the $(0,1^1,1)$e levels in the range $J = 9-13$ arise through interaction with e levels of the $(0,4^2,0)$ state. Probably for intensity reasons, no perturbations were found in the emission spectra of CdD_2 isotopomers.[6] However, our calculations yielded various perturbations for the doubly deuterated species, the lowest lying ones occurring between $(0,1^1,1)$e and $(0,4^4,0)$e levels.

A rather complex picture of perturbations is predicted for CdH_2 isotopomers in the region of the Darling−Dennison resonance system $(2,0^0,0)/(0,0^02)$. As many as eight interacting states are involved and without help from theory spectroscopists will hardly be able to untangle such a complex situation. A larger body of experimental information is available for $^{64}ZnH_2$ and $^{64}ZnD_2$ and current work is devoted to the analysis of various perturbations in these species.[35]

Acknowledgment. Financial support from the Deutsche Forschungsgemeinschaft (DFG) and from the Fonds der Chemischen Industrie is gratefully acknowledged.

Supporting Information Available: Eight tables with spin−orbit contributions (S1), total energy and dipole moment values (S2−S5) and rovibrational term energies of interacting levels (S6−S8) plus five figures showing calculated absorption spectra. This material is available free of charge via the Internet at http://pubs.acs.org.

References and Notes

(1) Andrews, L. *Chem. Soc. Rev.* **2004**, *33*, 123.
(2) Körsgen, H.; Urban, W.; Brown, J. M. *J. Chem. Phys.* **1999**, *110*, 3861.
(3) Shayesteh, A.; Yu, S.; Bernath, P. F. *Chem.−Eur. J.* **2005**, *11*, 4709.
(4) Shayesteh, A.; Gordon, I. E.; Appadoo, D. R. T.; Bernath, P. F. *Phys. Chem. Chem. Phys.* **2005**, *7*, 3132.
(5) Shayesteh, A.; Gordon, I. E.; Appadoo, D. R. T.; Bernath, P. F. *Phys. Chem. Chem. Phys.* **2006**, *8*, 3796.
(6) Yu, S.; Shayesteh, A.; Bernath, P. F. *J. Chem. Phys.* **2005**, *122*, 194301.
(7) Shayesteh, A.; Bernath, P. F. *J. Phys. Chem. A* **2005**, *109*, 10280.
(8) Greene, T. M.; Brown, W.; Andrews, L.; Downs, A. J.; Chertihin, G. V.; Runeberg, N.; Pyykkö, P. *J. Phys. Chem. A* **1995**, *99*, 7925.
(9) Wang, X.; Andrews, L. *J. Phys. Chem. A* **2004**, *108*, 11006.
(10) Raghavachari, K.; Trucks, G. W.; Pople, J. A.; Head-Gordon, M. *Chem. Phys. Lett.* **1989**, *157*, 479.
(11) Figgen, D.; Rauhut, G.; Dolg, M.; Stoll, H. *Chem. Phys.* **2005**, *311*, 227.
(12) Peterson, K. A.; Puzzarini, C. *Theor. Chem. Acc.* **2005**, *114*, 283.
(13) Dunning, T. H., Jr. *J. Chem. Phys.* **1989**, *90*, 1007.
(14) Kendall, R. A.; Dunning, T. H., Jr.; Harrison, J. *J. Chem. Phys.* **1992**, *96*, 6796.
(15) Woon, D. E.; Dunning, T. H., Jr. *J. Chem. Phys.* **1993**, *98*, 1358.
(16) Werner, H.-J.; Knowles, P. J. *MOLPRO*, version 2006.1, a package of ab initio programs; Lindh, R., Schütz, M., Celani, P., Korona, T., Manby, F. R., Rauhut, G., Amos, R. D., Bernhardsson, A., Berning, A., Cooper, D. L., Deegan, M. J. O., Dobbyn, A. J., Eckert, F., Hampel, C., Hetzer, G., Lloyd, A. W., McNicholas, S. J., Meyer, W., Mura, M. E. , Nicklass, A., Palmieri, P., Pitzer, R., Schumann, U., Stoll, H., Stone, A. J., Tarroni, R., Thorsteinsson, T., contributors; see http://www.molpro.net.
(17) Hampel, C.; Peterson, K.; Werner, H.-J. *Chem. Phys. Lett.* **1992**, *90*, 1.
(18) Botschwina, P.; Sebald, P.; Figgen, D.; Stoll, H. *Mol. Phys.* **2007**, *105*, 1193.
(19) Yabushita, S.; Zhang, Z.; Pitzer, R. M. *J. Phys. Chem. A* **1999**, *103*, 5791.
(20) Lischka, H.; Shepard, R.; Shavitt, I.; Pitzer, R. M.; Dallos, M.; Müller, Th.; Szalay, P. G.; Brown, F. B.; Ahlrichs, R.; Böhm, H. J.; Chang, A.; Comeau, D. C.; Gdanitz, R.; Dachsel, H.; Ehrhardt, C.; Ernzerhof, M.; Höchtl, P.; Irle, S.; Kedziora, G.; Kovar, T.; Parasuk, V.; Pepper, M. J. M.; Scharf, P.; Schiffer, H.; Schindler, M.; Schüler, M.; Seth, M.; Stahlberg, E. A.; Zhao, G.-G.; Yabushita, S.; Zhang, Z. COLUMBUS, release 5.8, an ab initio Electronic Structure Program, 2001.
(21) Lee, T. J.; Taylor, P. R. *Int. J. Quantum Chem. Symp.* **1989**, *23*, 199.
(22) Meyer, W.; Botschwina, P.; Burton, P. *J. Chem. Phys.* **1986**, *84*, 891.
(23) Watson, J. K. G. *Mol. Phys.* **1970**, *19*, 465.
(24) Sebald, P. Dissertation, Kaiserslautern, 1990.
(25) Nielsen, H. H. *Rev. Mod. Phys.* **1951**, *23*, 90.
(26) Nielsen, H. H. In *Encyclopedia of Physics*; Flügge, S., Ed.; Springer: Berlin, 1959; Vol. XXXVII/1, pp 173.
(27) Amat, G.; Nielsen, H. H.; Tarrago, G. *Rotation-Vibration of Polyatomic Molecules*; Dekker: New York, 1971.
(28) Carter, S.; Senekowitsch, J.; Handy, N. C.; Rosmus, P. *Mol. Phys.* **1987**, *65*, 143.
(29) Watson, J. K. W. *J. Mol. Spectrosc.* **1987**, *125*, 428.
(30) Botschwina, P. *Chem. Phys.* **1983**, *81*, 73, and references therein.
(31) Darling, B. T.; Dennison, D. M. *Phys. Rev.* **1940**, *57*, 128.
(32) Watson, J. K. G. *Can. J. Phys* **2001**, *79*, 521, and references therein.
(33) Botschwina, P.; Oswald, M.; Sebald, P. *J. Mol. Spectrosc.* **1992**, *155*, 360.
(34) Watson, J. K. G. *J. Mol. Spectrosc.* **1983**, *101*, 83.
(35) Sebald, P.; Botschwina, P. Unpublished.

JP9029198